

Supporting Information

BaTiO₃-g-GO as an efficient permselective material for lithium-sulfur batteries

Paulina Pórolnickzak¹, Mariusz Walkowiak^{1*}, Justyna Kaźmierczak-Raźna¹, Dawid Kasprzak¹, Deepa Elizabeth Mathew^{2,3}, M. Kathiresan^{2*}, A. Manuel Stephan^{2*}, N. Angulakshmi¹

¹ Łukasiewicz Research Network - Institute of Non-Ferrous Metals, Division in Poznań,
Central Laboratory of Batteries and Cells, Forteczna 12 St., 61-362 Poznań, Poland.

² CSIR- Central Electrochemical Research Institute, Karaikudi 630 003, India

³ Academy of Scientific and Innovative Research (AcSIR), Ghaziabad- 201002, India.

*Corresponding authors

Tel: +91 4565 241426 Fax: +91 4565 2777

e-mail: amstephan@cecri.res.in,

mariusz.walkowiak@claio.poznan.pl

kathir.org@gmail.com

Synthesis of BaTiO₃-g-GO

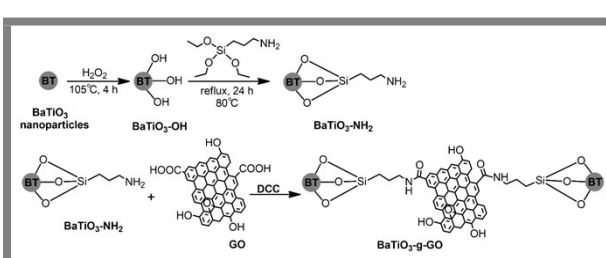


Figure SI 1a. Synthesis of BaTiO₃-g-GO.

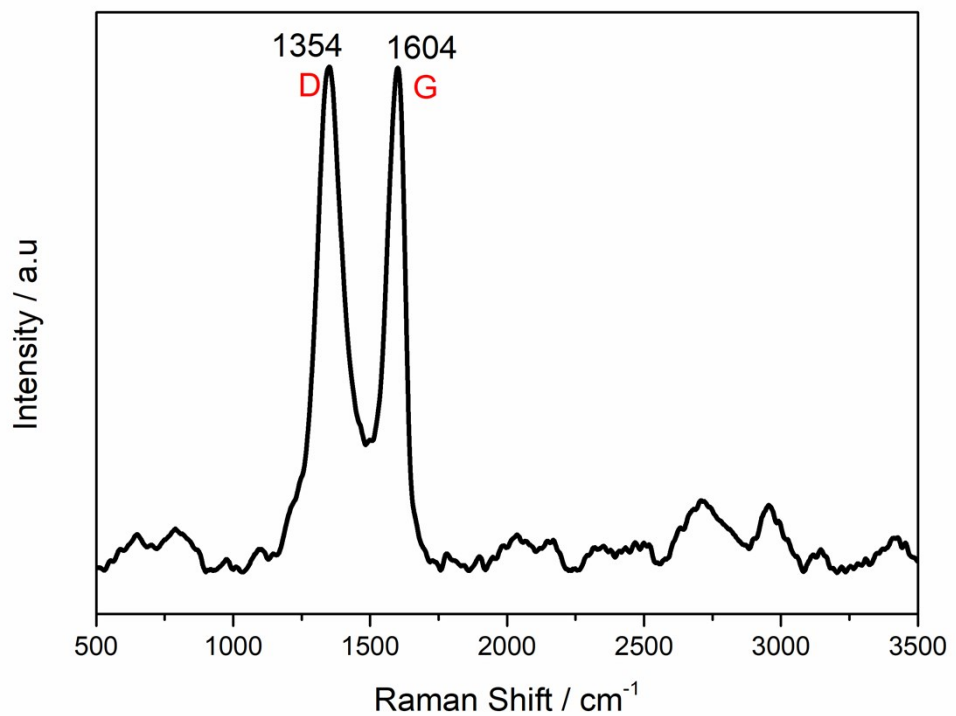


Figure SI 1b. Raman spectrum of synthesized Graphene Oxide.

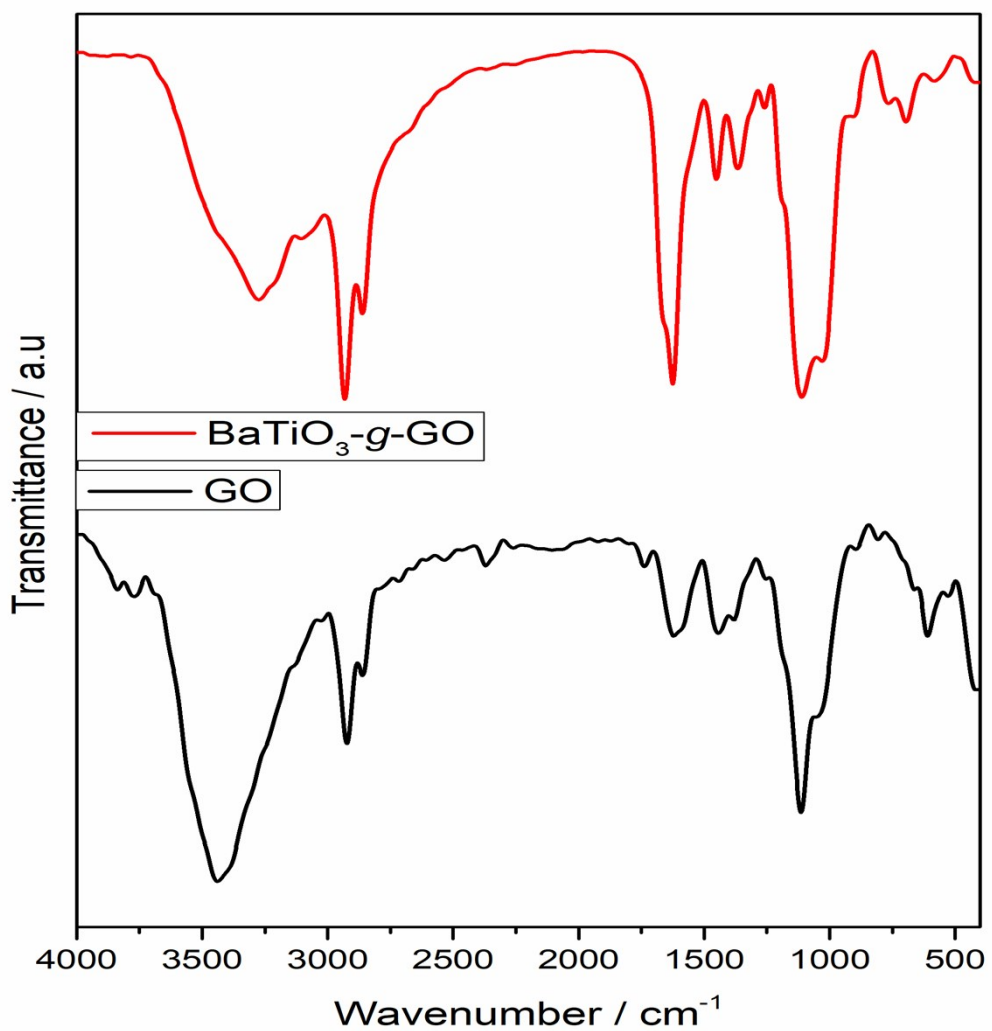


Figure SI 1c. The FT-IR spectra of GO and BaTiO₃-g-GO

EDX

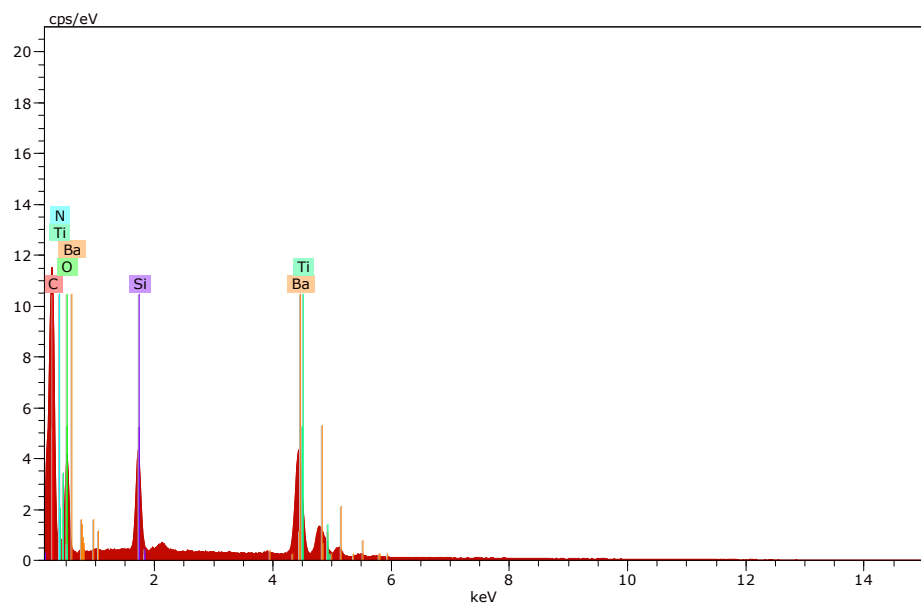


Figure SI 1d. EDX spectrum of synthesized BaTiO₃-g-GO.

Spectrum: Acquisition 9811

E1 AN Series unn. C norm. C Atom. C Error (1 Sigma) K fact. Z corr. A corr. F corr.

[wt.%]	[wt.%]	[at.%]	[wt.%]
--------	--------	--------	--------

Ba 56 L-series 1.028	43.90	41.41	6.47	1.30	0.320	1.258	1.000
C 6 K-series 1.000	42.35	39.95	71.37	4.98	0.766	0.521	1.000
O 8 K-series 1.000	14.53	13.71	18.38	1.92	0.165	0.829	1.000
Si 14 K-series 1.008	5.24	4.94	3.78	0.25	0.028	1.726	1.000
Ti 22 K-series 1.083	0.00	0.00	0.00	0.00	0.000	0.000	1.000
N 7 K-series 1.000	0.00	0.00	0.00	0.00	0.000	0.000	1.000

Total: 106.03 100.00 100.00

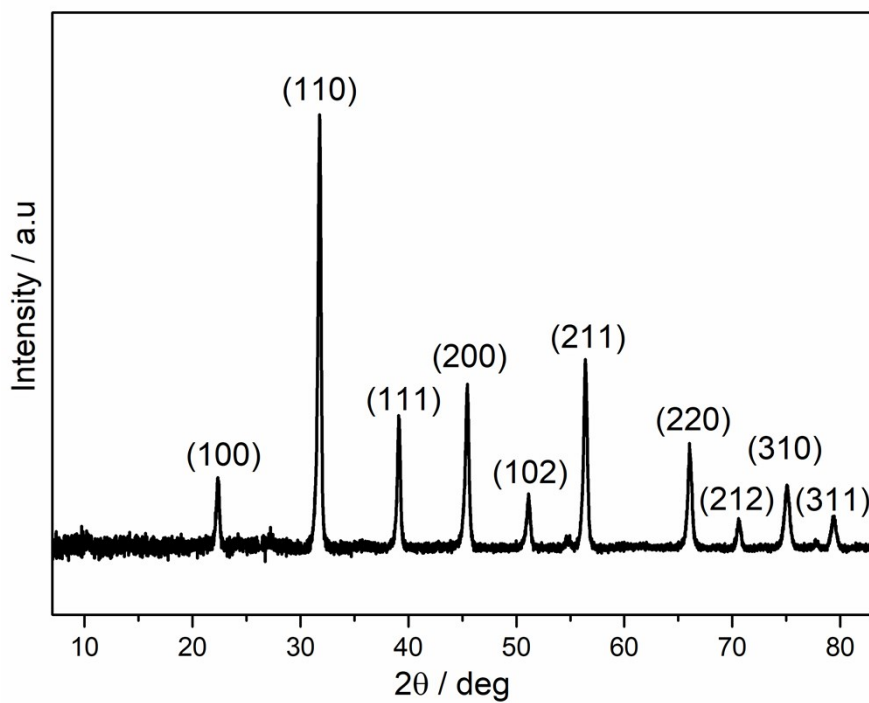


Figure SI 1e. XRD spectrum of BaTiO₃-g-GO

XRD spectrum of BaTiO₃-g-GO showed characteristic peaks of BaTiO₃. Since GO constitutes only 0.3 wt%, GO peaks are not visible in XRD. Diffraction peaks for BaTiO₃ nanoparticles were observed at 2θ 22.38°, 31.78°, 39.15°, 45.42°, 51.14°, 56.41°, 66.08°, 70.68°, 75.07°, and 79.42° and these peaks signify the Bragg reflections from the (100), (110), (111), (200), (102), (211), (220), (212), (310), and (311) planes correspondingly.¹ The obtained XRD pattern matches well with the standard XRD pattern of BaTiO₃ particle [JCPDS card no. 79-2264].

SEM images of Ba-TiO₃-g-GO

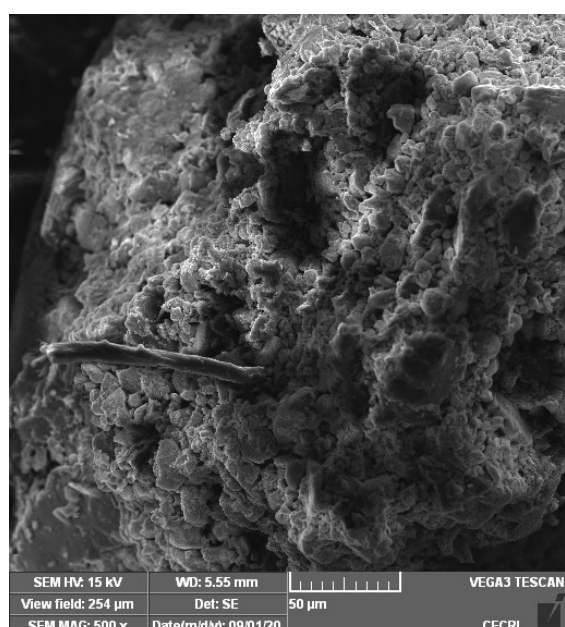
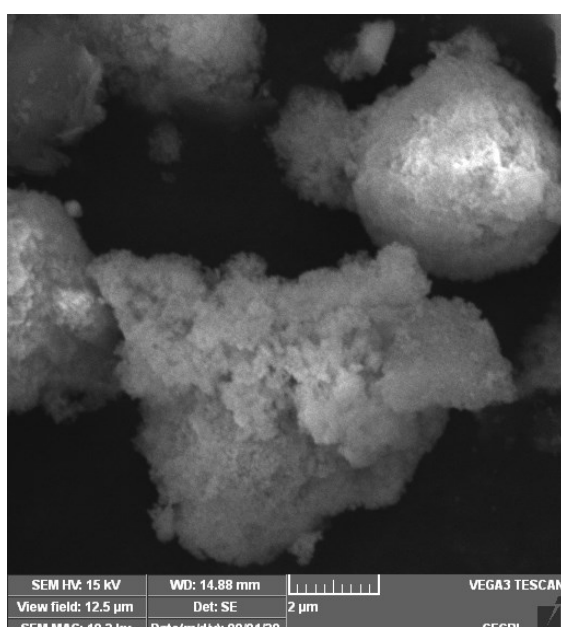
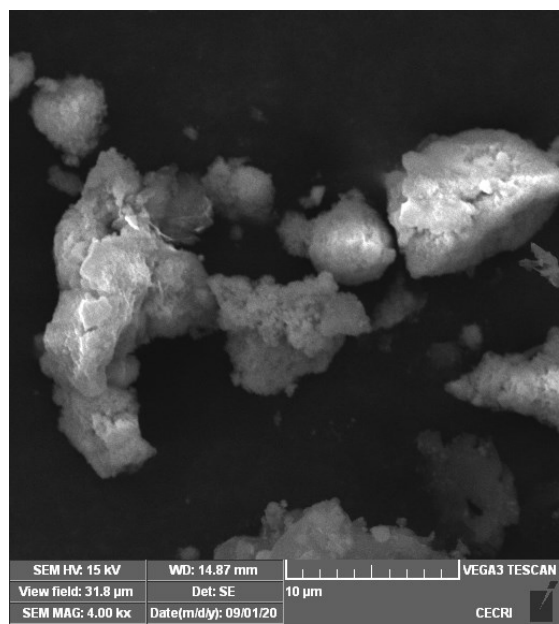
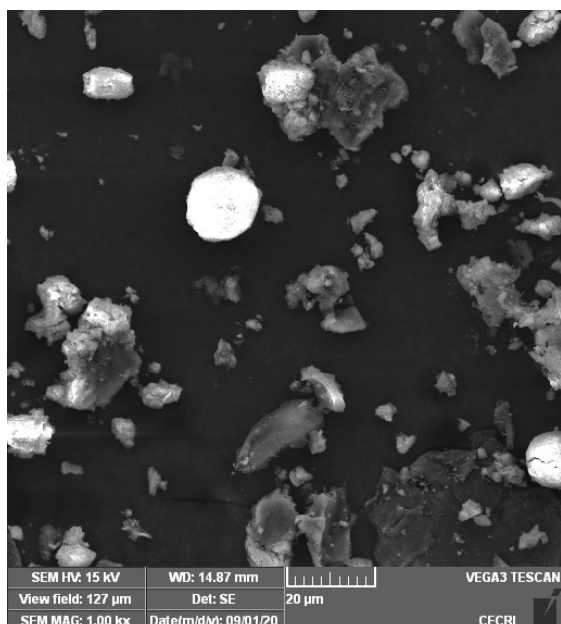


Figure SI 1f. SEM images of BaTiO₃-g-GO at different magnifications

XPS spectrum of synthesized BaTiO₃-g-GO

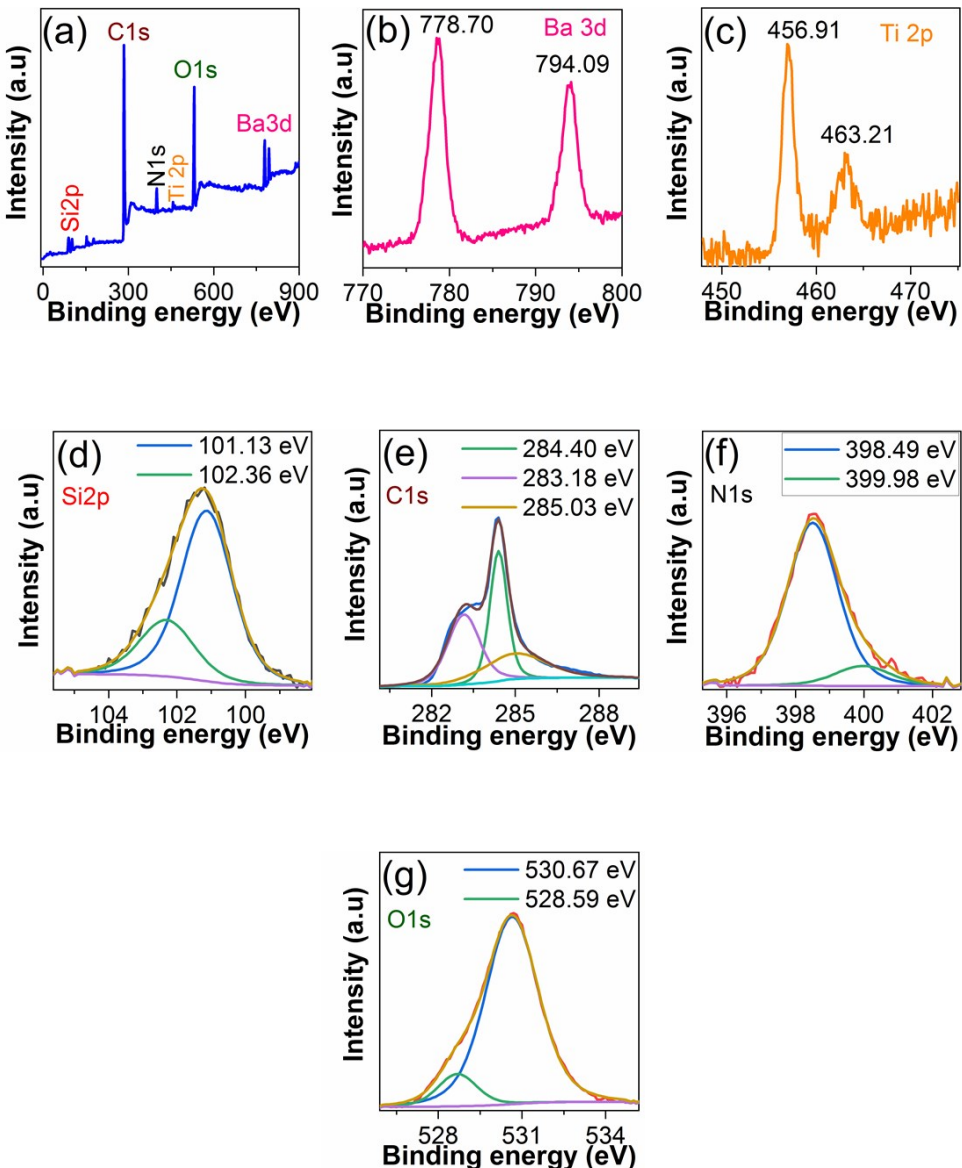


Figure SI 1g. XPS spectrum of the as synthesized BaTiO₃-g-GO a) Survey spectrum, b) Ba 3d spectra, c) Ti 2p spectra, d) Si 2p spectra, e) C 1s spectra, f) N 1s spectra and g) O 1s spectra.

The XPS survey spectrum shows evident peaks of C, O, N, Si, Ba, and Ti (Figure SI 1g-a) indicating the existence of BaTiO₃, linking APTS, and GO.

- The two peaks at 778.7 and 794.09 eV are ascribed to the splitting of Ba 3d_{5/2} and Ba 3d_{3/2} spin states correspondingly (Figure SI 1g-b).
- Two bands at 456.91 and 463.21 eV are ascribed to Ti 2p_{3/2} and Ti 2p_{1/2} respectively.
- Si 101.13, 102.36 eV corresponds to Si-O and SiO₂ respectively.

- C 1s 284.40 eV indicates the presence of C-C/C=C, 283.18 assigned to C-C/C-H and 285.03 eV to presence of C-O bond, all of which corresponds to GO.
- N 1s -398.49 eV attributed to N-H in amine, and 399.98 eV ascribed to N-C single bonds.
- 530.67 eV assigned to C-O bond, and 528.59 eV assigned to oxides (TiO, SiO).

All these results clearly indicate the existence of BaTiO₃-grafted graphene oxide interconnected via APTES linkage.

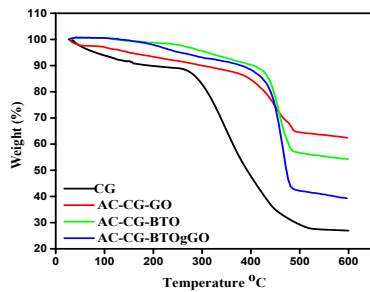


Figure SI 2. TG- curves for the coated membrane.

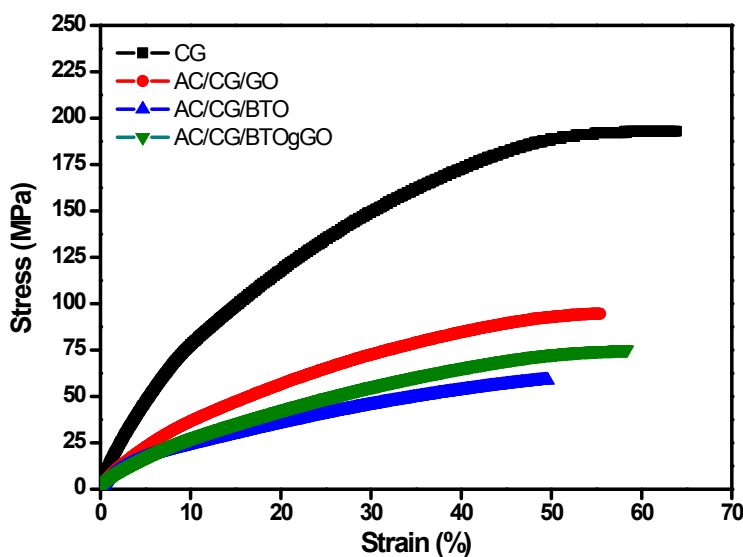


Figure SI 3. Stress- strain plot of Celgard 2320, AC/ GO, AC/BTO and AC/ BTO-g-GO coated trilayermembrane separators.

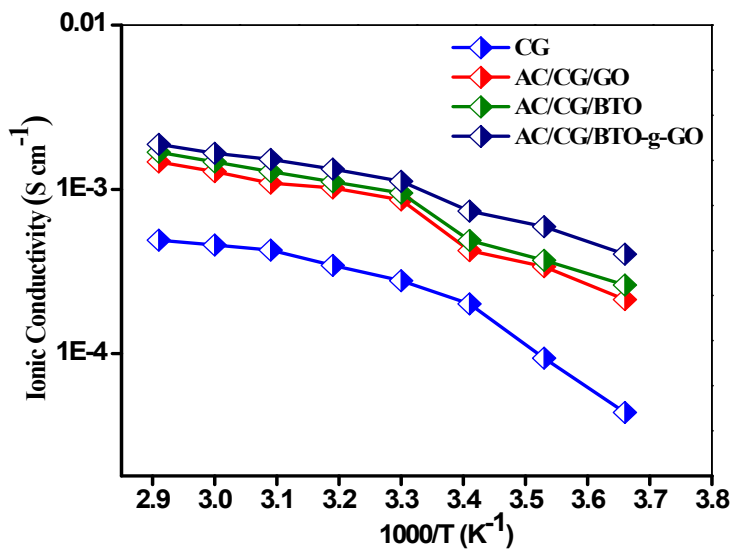


Figure SI 4. Variation of ionic conductivity as a function of inverse temperature.

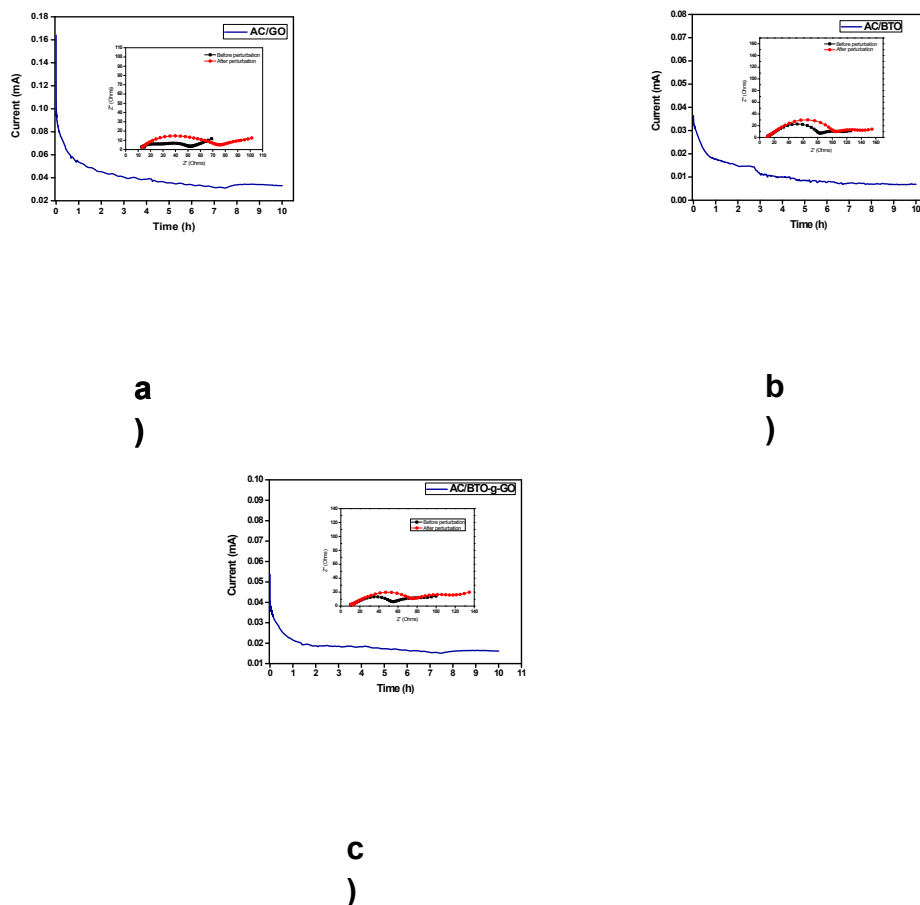


Figure SI 5. Chronoamperometric curve for the Li-S cells with a)AC/ GO, b) AC/BTO and c) AC/ BTO-g-GO after perturbation. **Inset:** Impedance spectra of the cell before and after DC polarization at room temperature.

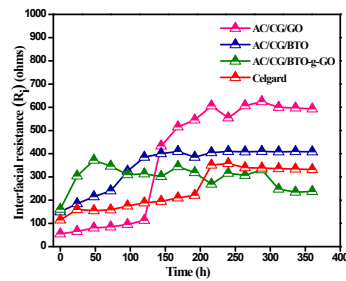


Figure SI 6. The variation of interfacial resistance as a function of time for Li/Separator/Li symmetric cells at room temperature.

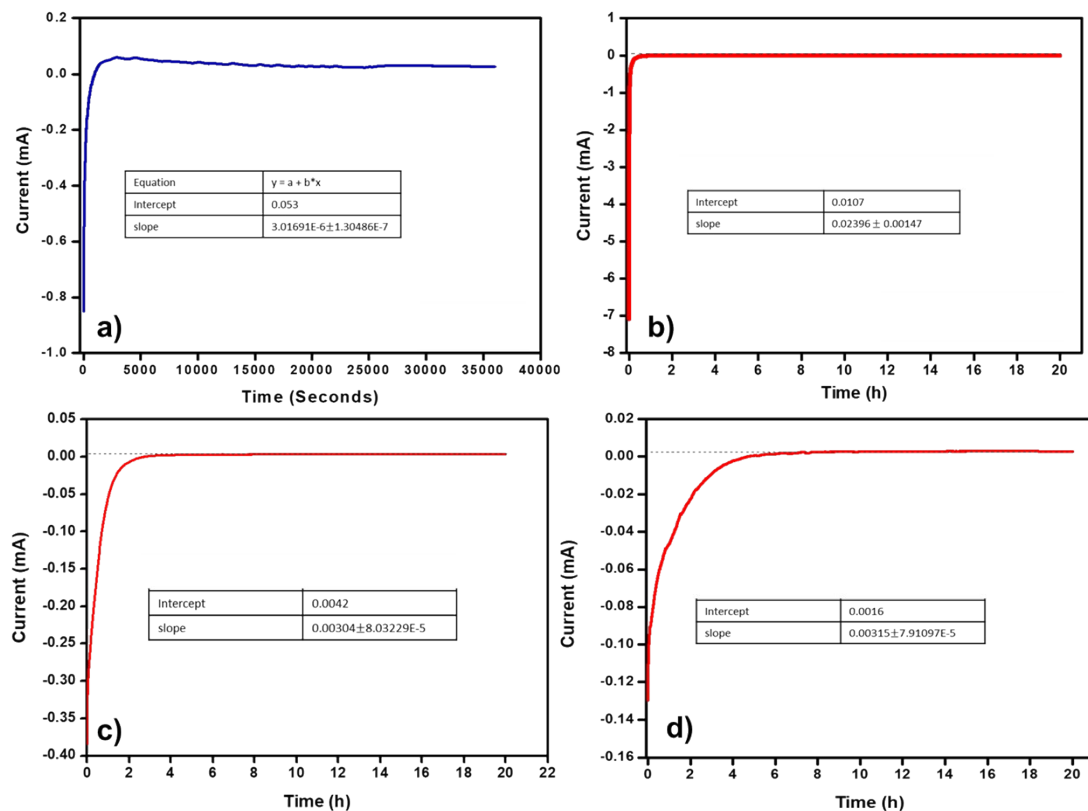
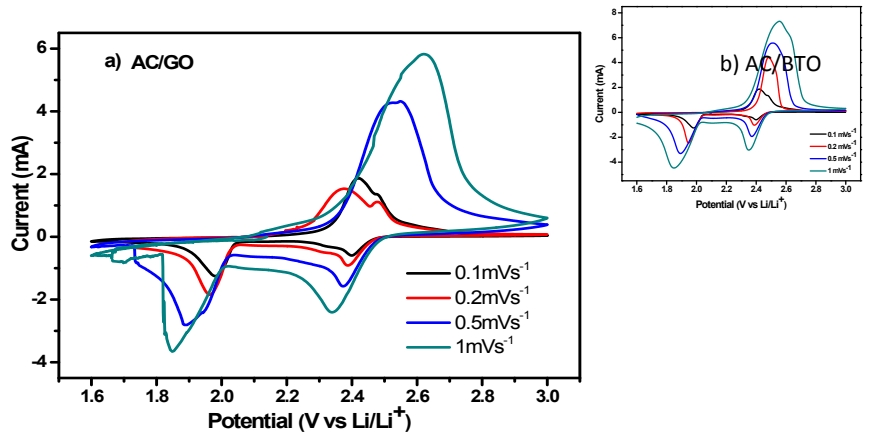
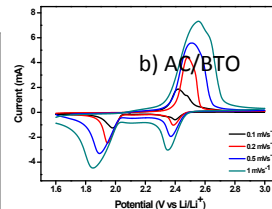


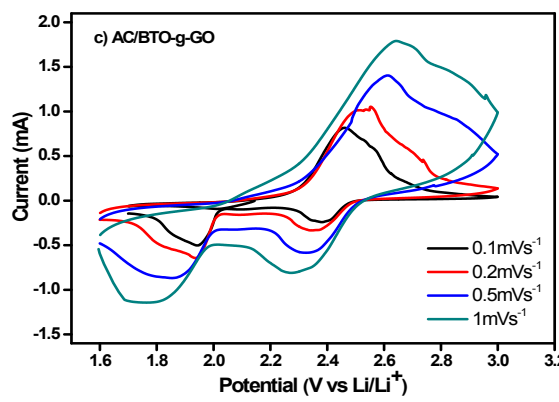
Figure SI 7. Current profile of Li-S cells with a) Celgard b) AC/GO c) AC/BTO d)AC/BTO-g-GO held at a constant potential of 2.3 V.



Peak	Diffusion coefficient (cm ² s ⁻¹)
2.4	5.1×10^{-5}
1.99	8.9×10^{-5}
2.4	3.02×10^{-6}
2.48	2.04×10^{-6}



Peak	Diffusion coefficient (cm ² s ⁻¹)
2.4	9.3×10^{-5}
1.99	1.02×10^{-6}
2.4	2.84×10^{-6}
2.48	2.6×10^{-6}



Peak	Diffusion coefficient (cm ² s ⁻¹)
2.4	5.31×10^{-4}
1.99	6.28×10^{-4}
2.4	1.47×10^{-5}
2.48	1.17×10^{-5}

Figure SI 8. The lithium-ion diffusion coefficients calculated for Li-S cells with a) AC/GO b) AC/BTO and d) AC/BTO-g-GO membranes.

Table 1. Comparison of permselective trilayer membranes properties with the present system

Sl. No	Sulfur content (wt%)	Mass loading of S electrode (mg/cm ²)	Thickness of the coating layer (μm)	Mass of the coating layer (mg/cm ²)	Initial discharge capacity (mAh/g)	Reversible discharge capacity (mAh/g)	No. of cycles	C rate	Degradation rate per cycle (%)	Reference
1	75	0.75	25	1.32	1067.7	804.4	100	0.2 C	1.3	2
2	80	2.5(areal loading)	35	1	1110.4	801.6	300	0.5	NA	3
3	60	1.4	8	0.01	1020	709	100	0.2	0.3	4
4	63	1.5	20	0.12	920	NA	100	0.1	0.49 to 0.23	5
5	60	1	25	0.5	836	610	200	0.1	0.1	6
6	72	0.72	47	0.8	1350	620	100	0.1	2.20	7
7	80	1	NA	NA	1045	628	50	0.05	1.6	8
8	42	1	42	NA	1287	807.8	100	0.2	1.60	9
9	80	0.7	20	0.825	1382	924	200	0.1	1.4	10
10	70	1.7	35	0.9	1382	1015	200	0.2	0.1	11
11	70	4	25	0.8	1450	833.3	100	0.1	0.6	12

Supporting References

- 1 S. Nayak, B. Sahoo, T. K. Chaki and D. Khastgir, *RSC Adv.*, 2014, **4**, 1212–1224.
- 2 R. Song, R. Fang, L. Wen, Y. Shi, S. Wang and F. Li, *J. Power Sources*, 2016, **301**, 179–186.
- 3 G. Ma, F. Huang, Z. Wen, Q. Wang, X. Hong, J. Jin and X. Wu, *J. Mater. Chem. A*, 2016, **4**, 16968–16974.
- 4 C. H. Chang, S. H. Chung and A. Manthiram, *J. Mater. Chem. A*, 2015, **3**, 18829–18834.
- 5 J. Q. Huang, T. Z. Zhuang, Q. Zhang, H. J. Peng, C. M. Chen and F. Wei, *ACS Nano*, 2015, **9**, 3002–3011.

- 6 H. Yao, K. Yan, W. Li, G. Zheng, D. Kong, Z. W. Seh, V. K. Narasimhan, Z. Liang and Y. Cui, *Energy Environ. Sci.*, 2014, **7**, 3381–3390.
- 7 M. Raja, S. Suriyakumar, N. Angulakshmi and A. Manuel Stephan, *Inorg. Chem. Front.*, 2017, **4**, 1013–1021.
- 8 X. Ou, Y. Yu, R. Wu, A. Tyagi, M. Zhuang, Y. Ding, I. H. Abidi, H. Wu, F. Wang and Z. Luo, *ACS Appl. Mater. Interfaces*, 2018, **10**, 5534–5542.
- 9 Q. Xu, G. C. Hu, H. L. Bi and H. F. Xiang, *Ionics (Kiel)*, 2015, **21**, 981–986.
- 10 W. Ahn, S. N. Lim, D. U. Lee, K. B. Kim, Z. Chen and S. H. Yeon, *J. Mater. Chem. A*, 2015, **3**, 9461–9467.
- 11 J. Balach, T. Jaumann, M. Klose, S. Oswald, J. Eckert and L. Giebel, *J. Phys. Chem. C*, 2015, **119**, 4580–4587.
- 12 The present work.